Syrtis Major: A Low-Relief Volcanic Shield

GERALD G. SCHABER

U.S. Geological Survey, Flagstaff, Arizona 86001

Viking orbiter images and earth-based radar elevation data have been used to document the volcanic geology of Syrtis Major and to reevaluate its physiographic setting. These data indicate that Syrtis Major is actually a very low relief, simple shield with a central caldera complex; arcuate segments of concentric grabens at the shield summit define the limits of a 280-km-diameter depression that is thought to have been created by foundering of a magma chamber. Lava flows with well-defined scarps are associated with two summit calderas; fissures and lava tubes are recognized on the shield flanks. The lava flows were deposited on volcanic ridged plains that do not display flow scarps. Compressional stresses acting on the shield were apparently greatest following the deposition of the ridged-plains unit but continued at a somewhat reduced rate after deposition of the younger lavas. The extremely low-relief shield of the Syrtis Major as well as other volcanic plains of intermediate age in the eastern hemisphere of Mars is in striking contrast to the giant shields of Tharsis Montes. Such different types of volcanic landforms may result from changes with times in the composition, differentiation history, eruption rates, and eruption temperatures of surface igneous rocks, thus, directly reflecting the thermal and chemical evolution of the interior. The low relief on the shields may also reflect a substantially thinner crust in these regions relative to Tharsis. The physiographic evidence and radar elevation data confirm the fact that Syrtis Major is a 'planum' (plateau) rather than a 'planitia' (low plain), as published maps of Mars now portray the feature. In addition, present evidence does not support an earlier suggestion that an impact basin predated volcanism at Syrtis Major.

Introduction

Viking orbiter images and earth-based radar elevation data have been used to map volcanic landforms at Syrtis Major Planitia and to reevaluate its geologic history and physiographic setting. These data have shown that Syrtis Major is a simple shield of very low relief that has a central caldera complex and generally circular plan. The shield appears to have been constructed on an old cratered plateau after formation by impact of the Isidis Basin (Isidis Planitia) to the east; no evidence has been found to support theories that an impact basin underlies the volcanic rocks at the Syrtis Major site [*Meyer and Grolier,* 1977; *Schultz and Glicken,* 1979]. The profile of the Syrtis Major shield appears to be similar to the profiles of all simple or complex shields on Mars that are old or intermediate in age. Other similar volcanic centers include the volcanic plains at Hesperia Planum and an extensive volcanic field in the Hellas basin region near Amphitrites Patera in the eastern hemisphere and Alba Patera in the western hemisphere [*Scott and Carr,* 1978]. Inferences can be made concerning planetary thermal evolution, crustal thickness differences, or changes in emplacement style, and composition of volcanic materials in Syrtis Major and the Tharsis region; the latter dominated by high-relief shields.

This report complements a recent study by *Simpson et al.* [1982] that describes radar measurements of small-scale surface roughness at Syrtis Major and correlates the roughness and surface slope data with geomorphic and eolian features as well as with thermal and bolometric albedo observations.

Geology of Central Syrtis Major

Photogeologic evaluation of Viking orbiter images of intermediate to high resolution (300 to 21 m per pixel) has resulted in recognition of extensive lava flows that extend outward from two calderas situated at the center of the Syrtis Major shield (Figures 1–3). The larger caldera (C_1) is 70 km in diameter and is breached on its southeast side (Figures 4 and 5); this vent was recognized and mapped by *Scott and Carr* [1978] from Mariner 9 images. Massed crescentic dunes with low albedo that were probably formed by easterly to northeasterly winds during an earlier more favorable climatic period on Mars [*Breed et al.,* 1979] have covered all impact craters in the region south of caldera C_1 [*Simpson et al.,* 1982] (Figures 3–6). The irregular appearance of the dune field's northeastern edge indicates that it is presently being eroded by northeasterly winds; these dunes may be the source for many of the abundant dark streaks and splotches that presently are visible west of the shield summit. The second caldera (C_2), 40 km in diameter, is about 150 km southeast of caldera C_1 (Figures 1–3 and 7–9). Lava channels or collapsed lava tubes extend radially from both calderas (Figures 7–10). Caldera C_1 contains a small volcanic cone whose east wall is breached (Figures 1 and 4–6). Both calderas are characterized by multiple concentric faults on their rims (Figures 1, 4, 5, and 7–10).

Segments of older, mostly buried, arcuate grabens have been recognized northeast and southwest of caldera C_1 and west of caldera C_2 (Figures 1, 3, and 4). These segments mark the perimeter of a 280-km-diameter circle centered between calderas C_1 and C_2; they are thought to represent the limits of a volcano-tectonic depression that formed when the roof of a magma chamber foundered after extensive extrusion of lava onto the surface.

The volcanic deposits forming the Syrtis Major shield spread over the cratered plateau west of the Isidis basin and into that depression in at least two eruptive stages. The first stage is represented by the extensive ridged-plains unit that now dominates the surface of the shield (Figure 1). There are no recognizable scarps on the lava flows of the ridged-plains unit. The second recognizable stage of volcanic activity in Syrtis Major is represented by the long, narrow lava flows

Paper number 2B0730.

hat extend
ıter of the
ɩera (C_1) is
theast side
mapped by
s. Massed
bly formed
ırlier more
1979] have
caldera C_1
lar appear-
es that it is
hese dunes
streaks and
shield sum-
s about 150
7–9). Lava
from both
all volcanic
4–6). Both
c faults on

abens have
:era C_1 and
segments
e centered
represent
rmed when
extensive

ajor shield
s basin and
s. The first
ıs unit that
. There are
dged-plains
activity in
lava flows

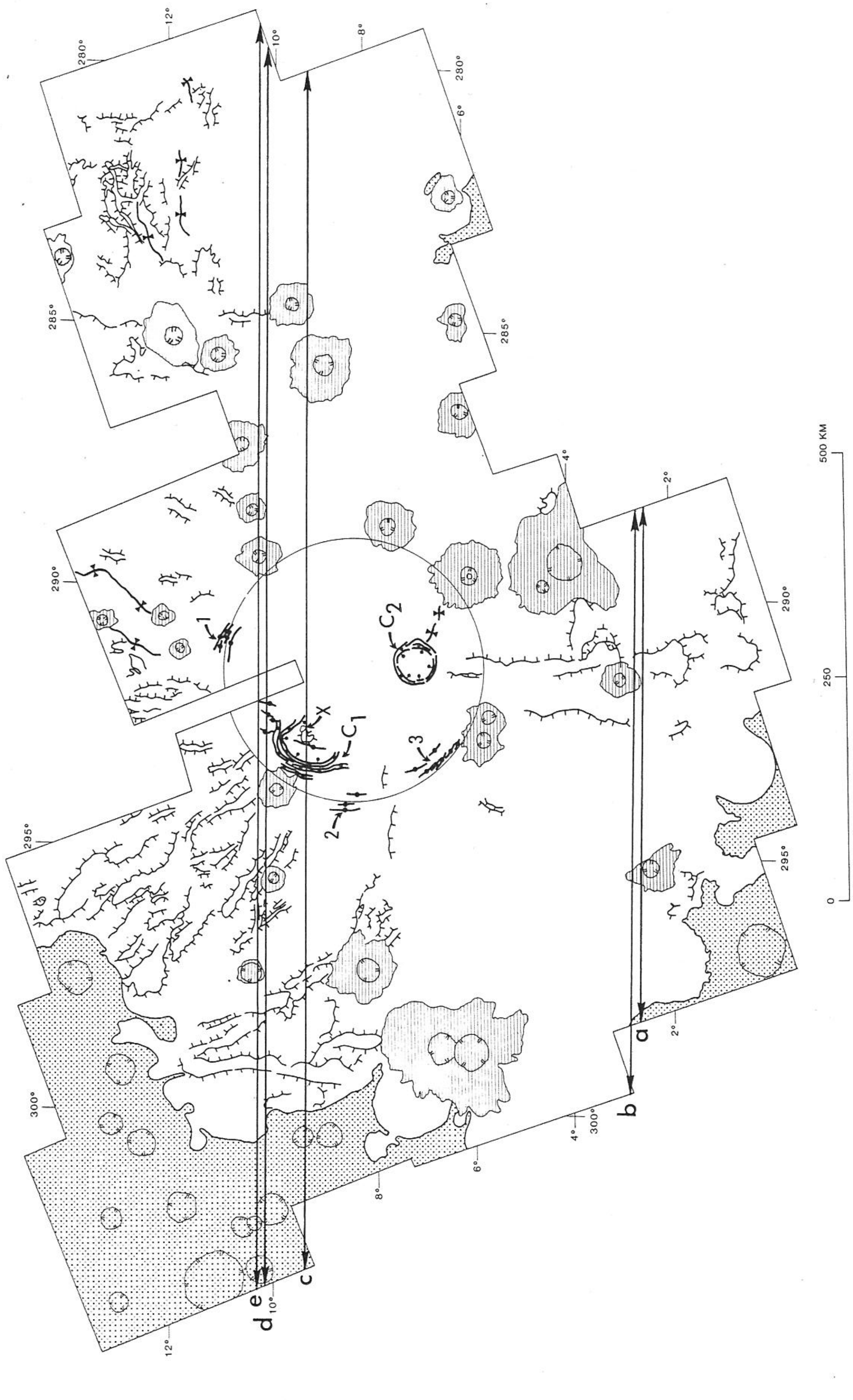

Fig. 1. Geologic sketch map of central Syrtis Major, showing cratered-plateau terrain (dotted pattern), ridged volcanic plains (blank), superposed craters (horizontal bars), lava flow scarps (hachured lines), fault grabens (heavy line with ball), and lava channels (line with bars pointed inward). Large circle surrounding calderas C_1 and C_2 represents limits of proposed summit depression discussed in text. The 1, 2, and 3 denote areas where segments of arcuate grabens lie on perimeter of 280-km-diameter depression (see Figure 3). The cross denotes location of small breached cone (see Figure 6). Subearth radar traces (a–e) show locations of radar profiles (Figure 13). Figure 2 shows photomosaic of map area. Geologic mapping compiled on mosaic of Viking orbiter images 375S08–375S13, 375S26–375S32, and 377S51–377S58. Average resolution, 219 m per pixel; solar illumination angle, 12° to 28°.

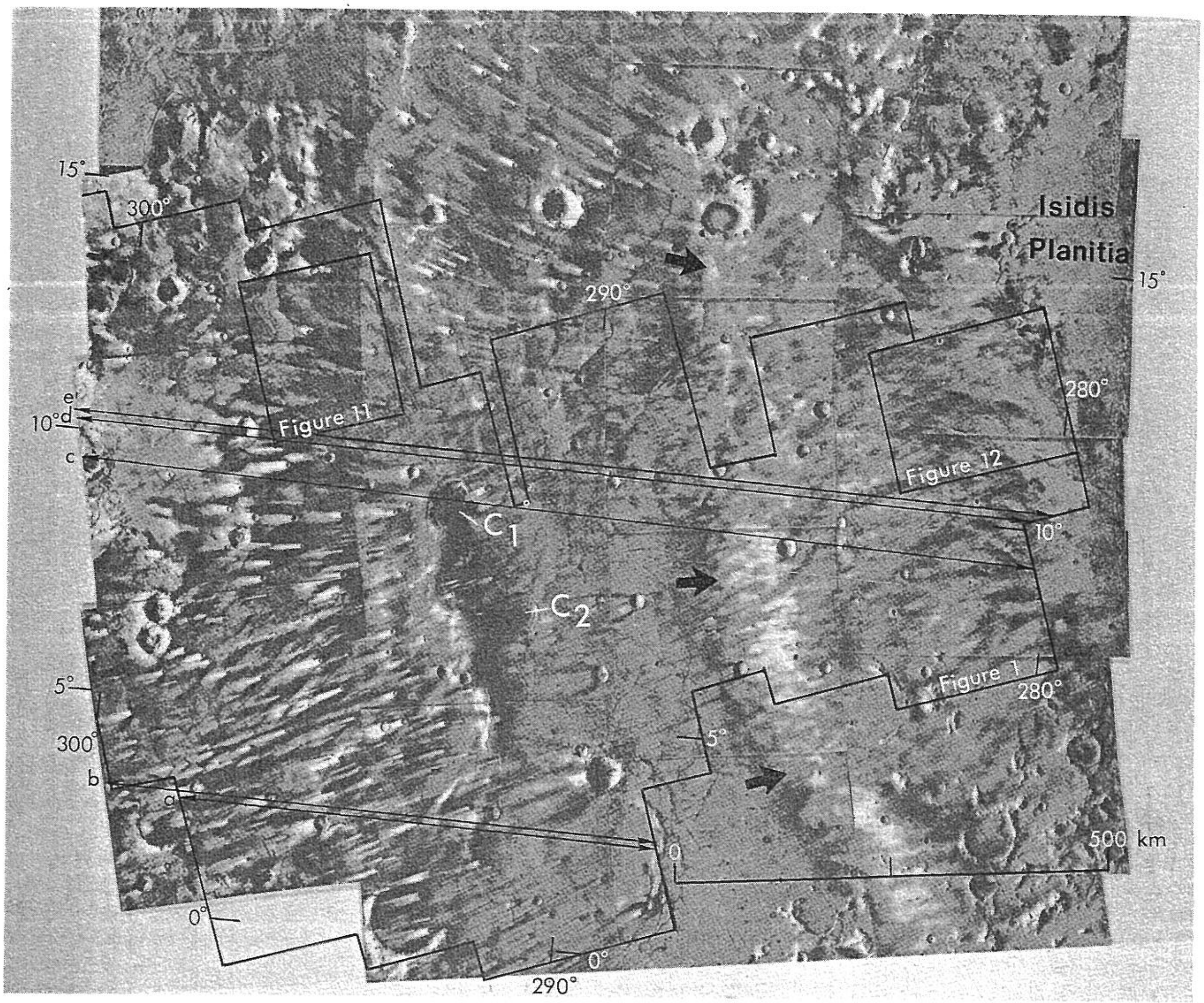

Fig. 2. Photomosaic of Viking orbiter images 496A45–496A52 and 496A65–496A74, showing Syrtis Major region from latitude 0° to 20°N, longitude 278° to 300°. Locations of Figures 1, 11, and 12 and radar elevation profiles a–e are also shown. Arrows indicate position where eastward slope (0.8°) into Isidis Planitia begins; note change in surface albedo on slope. Average resolution, 310 m per pixel; solar illumination angle, 11° to 27° from east to west.

shown in Figures 1 and 11. Compressional stresses acting on the shield were apparently greatest during the period after the ridged plains were deposited, but photogeologic data indicate that ridges continued to form at a somewhat reduced rate after deposition of the younger lava flows (Figure 11).

Lava flows with well-defined scarps have been mapped as much as 350 km northeast, north, and northwest of caldera C_1 and south of caldera C_2 (Figures 1 and 11); additional flow scarps have been mapped (Figure 1) about 650 km northeast of caldera C_1. Sources for these flank eruptives have been identified as a fissure vent and a collapsed lava tube that appear to originate near latitude 12°N, longitude 284° and extend eastward along the regional slope toward the floor of the Isidis basin (Figure 12).

Individual lava flows within Syrtis Major can be traced as far as 100 km and are as much as 20 km wide. The thickness of individual flows cannot be determined with certainty because the solar illumination was high, but height estimates range from 10 to 30 m (D. W. G. Arthur, personal communication, 1981). The general morphology of the Syrtis Major lavas resembles that of flows in the Tharsis Montes region, described by *Schaber et al.* [1978] and *Scott and Tanaka* [1981]. The age of individual flows cannot be distinguished by conventional crater-count methods from that of the underlying ridged plains, values for the entire Syrtis Major region average about 2000 craters >1 km in diameter per 10^6 km^2. This value agrees excellently with the crater count statistics given by *Simpson et al.* [1982] for Syrtis Major. The numbers of superposed impact craters are about the same for Syrtis Major volcanic materials as for the intermediate-stage lavas at Alba Patera, the earliest eruptives rocks associated with Arsia Mons, and the lava plains at Lunae Planum, Syria Planum, and Hesperia Planum [*Scott and Carr,* 1978; *Scott and Tanaka,* 1981; *Scott,* this issue].

RELATION OF TOPOGRAPHY TO ALBEDO VARIATIONS

The relation of low albedo to topography at Syrtis Major has been the subject of considerable debate in the past

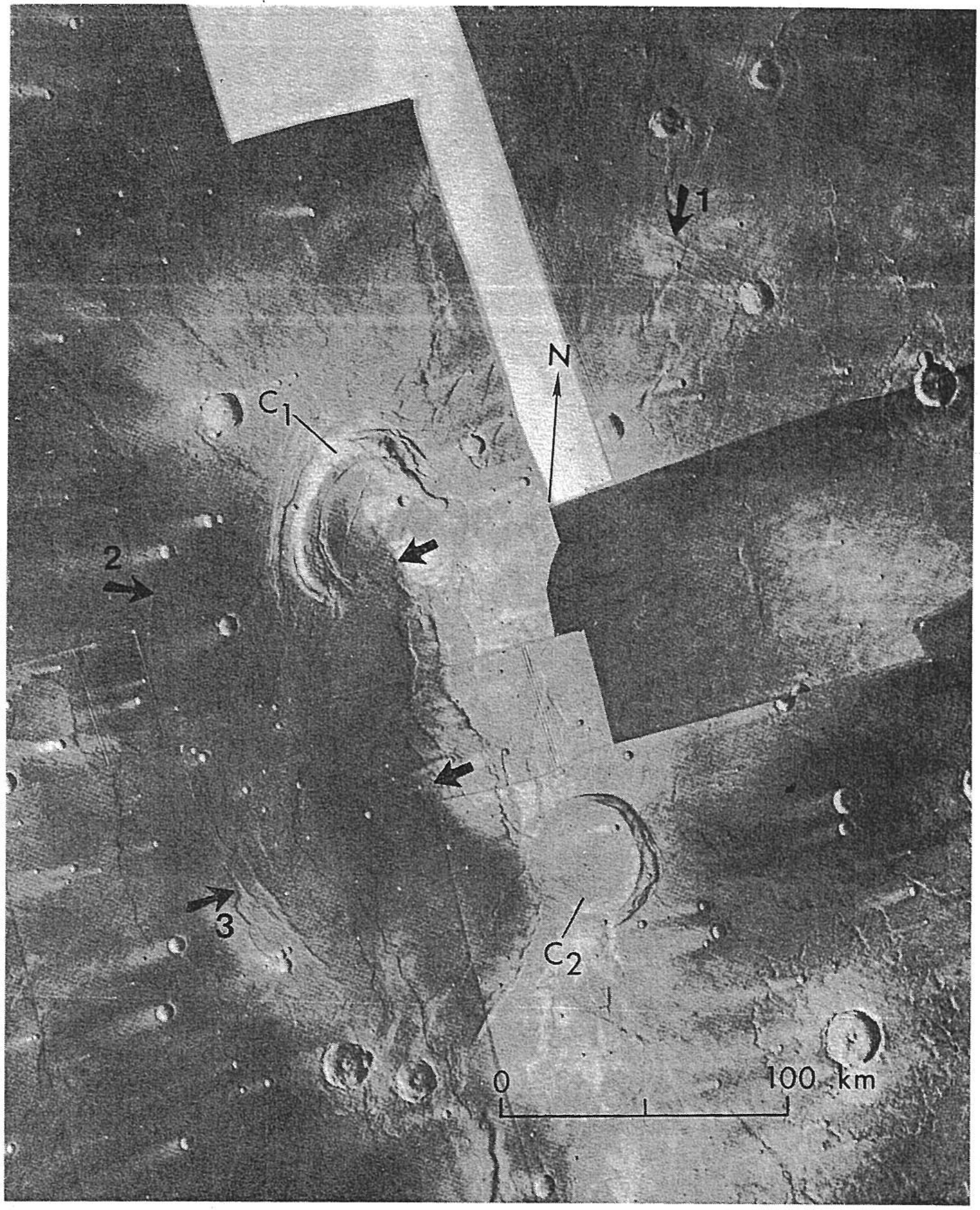

Fig. 3. Enlarged section of Viking orbiter mosaic used to compile geologic sketch map (Figure 1), showing summit calderas C_1 and C_2 and locations segments of arcuate grabens (1, 2, 3). Arrows between C_1 and C_2 mark edge of extensive crescentic dune field (Figures 5 and 6). Viking orbiter images used in mosaic include 375S12, 375S13, 375S28, 375S30, 375S32, 377S51 and 377S52. Average image resolution, 219 m per pixel; solar illumination angle, 12° to 28°.

[*Pollack and Sagan,* 1967, 1970; *Belton and Hunten,* 1969, 1971; *Wells,* 1969; *Goldstein et al.,* 1970; *Rogers et al.,* 1970; *Sagan et al.,* 1971; *Frey,* 1974]. Although Syrtis Major is historically one of the most persistent dark features on Mars, seasonal changes in its overall appearance were first described by *Antoniadi* [1930] and later verified by *Slipher* [1962]. *Antoniadi* [1930] reported, on the basis of 66 years of observational data, that Syrtis Major showed definite seasonal variations in size and albedo; it appeared narrow after perihelion and broad after aphelion, the changes occurring during northern autumn and spring, respectively [*Capen,* 1976]. *Antoniadi* [1930] emphasized that albedo changes along its east boundary (with Libya and Isidis Regio) drastically changed the size of Syrtis Major, whereas its west boundary (with Aeria) always remained rather stable. The observations by *Slipher* [1962] confirmed the variability of the east border of Syrtis Major. On the basis of early earth-based radar observations of Mars obtained during the 1963 and 1967 oppositions, *Sagan and Pollack* [1968] and *Sagan et al.* [1971] suggested that yellow clouds on Mars, which preferentially move through lowland areas, are deflected when they encounter highland areas or slopes. *De Vaucouleurs* [1954] and *Slipher* [1962] described several occasions when yellow clouds moved southward along Syrtis Major from Isidis Regio to Libya toward Hesperia.

Earth-based radar elevation profiles across Syrtis Major

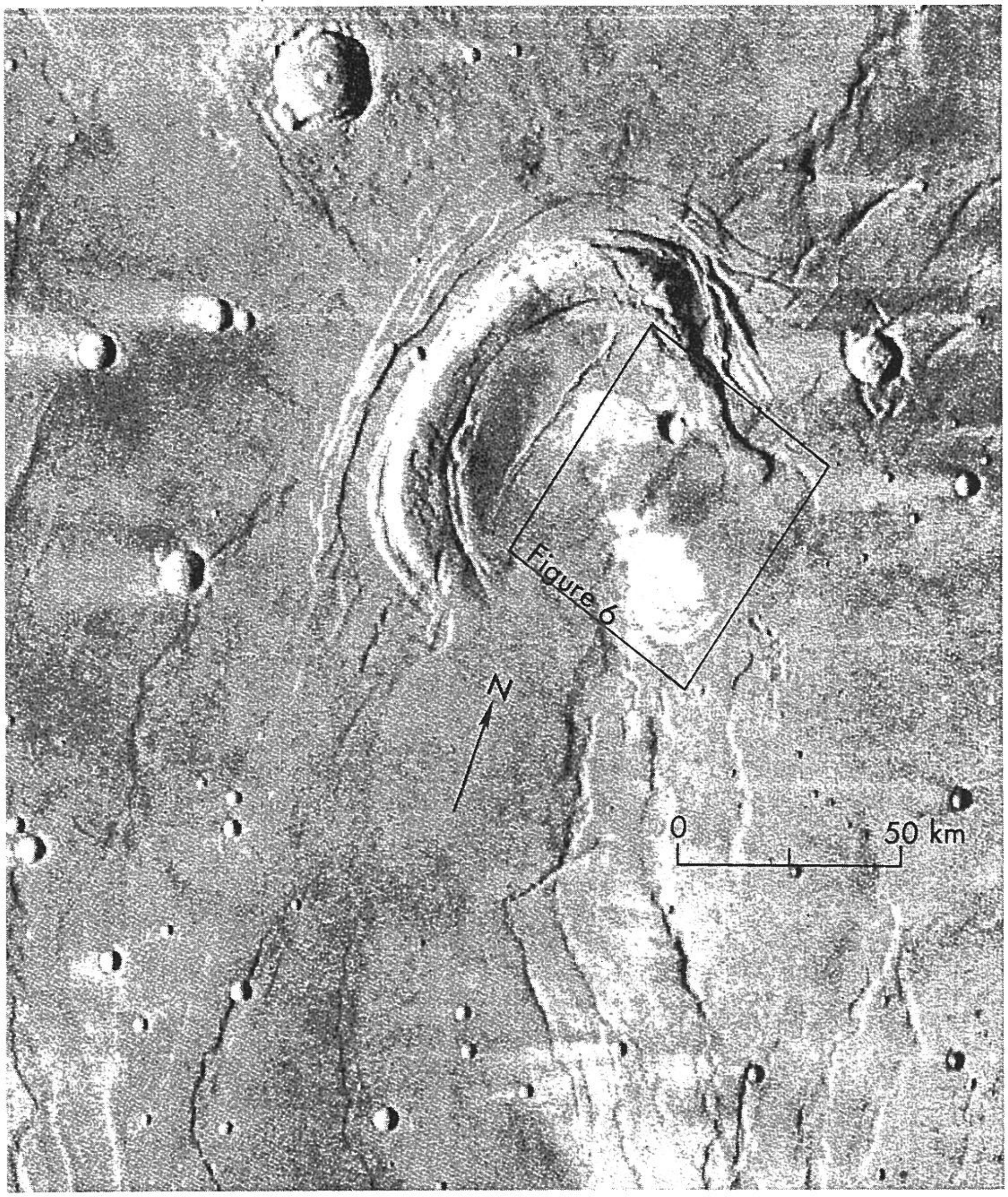

Fig. 4. Enlargement of Viking orbiter image 375S13 showing summit caldera C_1 and footprint of Figure 6. Image resolution, 221 m per pixel; solar illumination angle, 28°.

obtained in 1969 and 1975 [*Goldstein et al.*, 1970; *Rogers et al.*, 1970; *Downs et al.*, 1978] and measurements of elevation obtained by earth-based or spacecraft-borne CO_2 spectrometers [*Belton and Hunten*, 1969; *Wells*, 1969; *Hord et al.*, 1974] have demonstrated that Syrtis Major is a generally elevated plateau bordered by cratered highland terrain to the west and an east facing slope that falls off into Isidis Planitia. Estimates of the exact position and magnitude of this east facing slope differ in various published reports. *Rogers et al.* [1970] reported elevation differences of 5 km over 10° of longitude (from longitude 275° to longitude 285°) on the basis of earth-based radar observations during the 1969 opposition; during this same opposition, *Goldstein et al.* [1970] reported a nearly linear decrease in elevation of 4 km across Syrtis Major. A topographic map of Mars published by the *U.S. Geological Survey* [1976] and based on composite data sets that included Mariner 9 photogrammetry, earth-based radar, occultation, and infrared and ultraviolet data represents Syrtis Major as possessing a linear slope of 0.6° between longitude 279° and 300°, similar to that described by *Goldstein et al.* [1970].

Schaber et al. [1981] and *Simpson et al.* [1982] have recently described the topography across the center of Syrtis Major based on a single radar elevation profile obtained in 1978 at Arecibo, Puerto Rico. Figure 13 shows this profile (at latitude 10.33°N), together with other radar profiles obtained between 1975 and 1980 at Arecibo (Puerto Rico) and at Goldstone (California). These data clearly show the elevated character of the surface at Syrtis Major, and the increase in slope to 0.8° along its east border with Isidis Planitia,

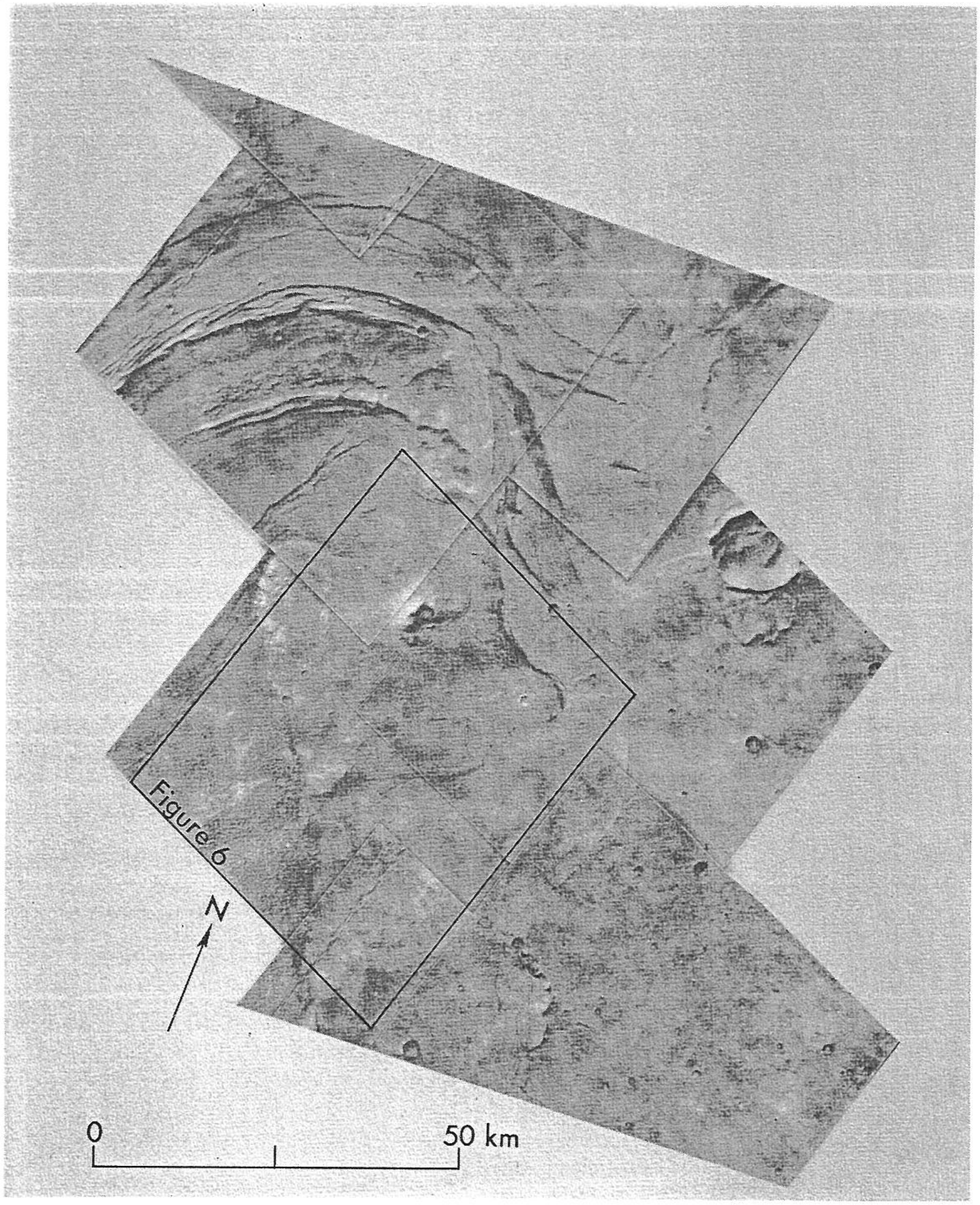

Fig. 5. Viking orbiter mosaic showing part of caldera C_1; mosaic includes 716A08–716A15. Image resolution, about 35 m per pixel; solar illumination angle, about 27°.

between longitude 285° and longitude 279°. It is now clear that long-term observations [*Antoniadi*, 1930; *Capen*, 1976] of conspicuous albedo changes along the eastern side of Syrtis Major are related to the presence of this rather significant slope (Figure 2 and 13).

Radar profile c (Figure 13) traverses the summit caldera C_1 and crosses the highest point on the shield [*Simpson et al.*, 1982]. This 280-km-diameter summit depression, recognized on the Viking orbiter images, can also be clearly identified in radar profiles d and e (Figure 13). A slight lateral discrepancy between the photogeologic position of the summit depression and the position indicated by the radar profiles is probably caused by slight variations in planetary figures used by the Goldstone and Arecibo groups, differing zero references for latitude and longitude, or errors in photolocation of the somewhat obscured eastern limit of the summit depression.

The size of the radar cell measured at the subradar point on the Martian surface varies with the radar facility. The radar cell measured by Goldstone is 0.16° to 0.50° (10 to 30 km) E-W and 2.6° to 4.0° (156 to 240 km) N-S; the Arecibo cell is 0.12° (6.9 km) E-W and 2.15° (127 km) N-S. These cells represent areas of 1560 to 7200 km^2 and 875 km^2, for Goldstone and Arecibo data, respectively (R. Simpson,

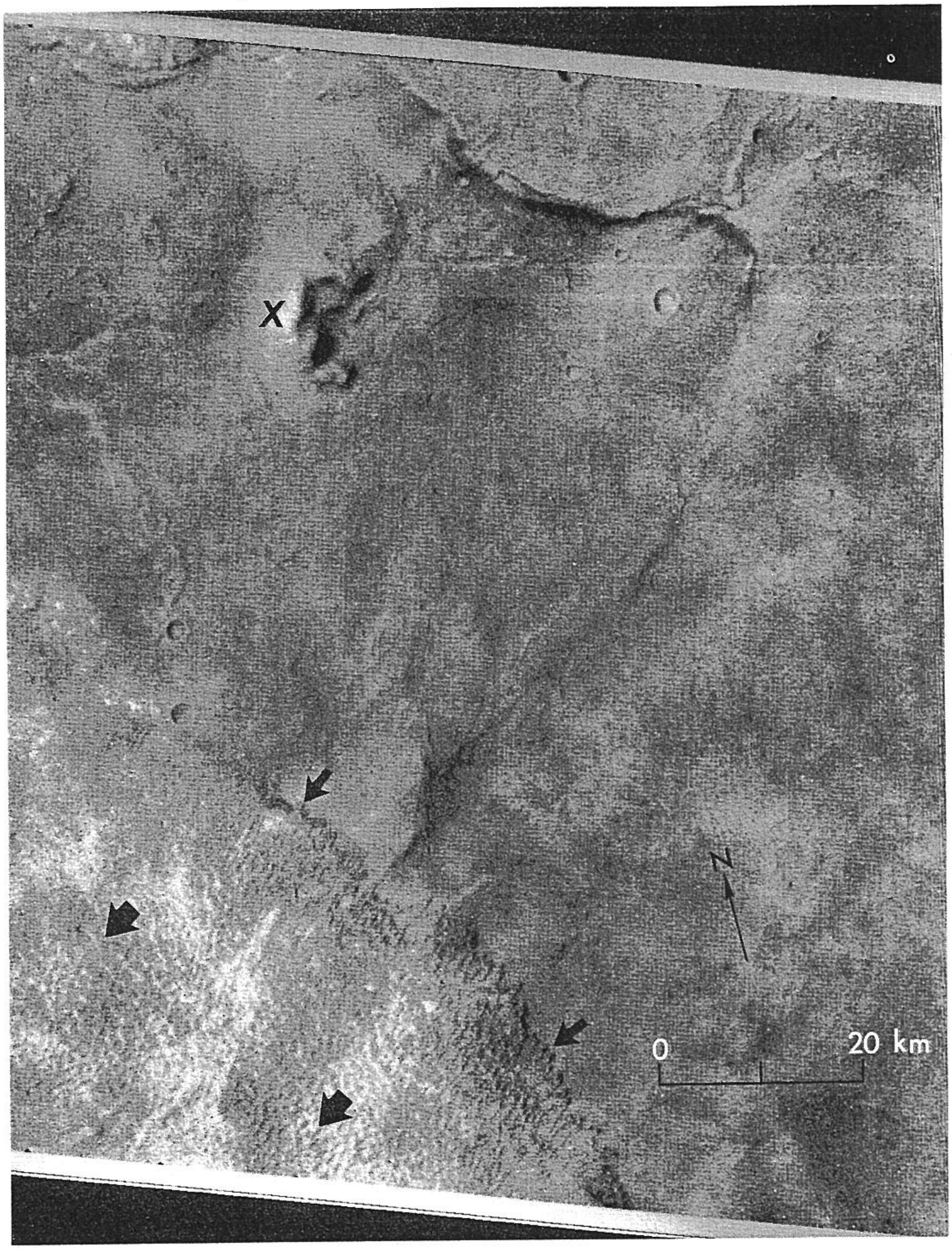

Fig. 6. Part of Viking orbiter image 716A12, enlarged to show erg (with massed crescentic dunes) south of caldera C_1 and breached volcanic cone (cross) (see Figure 5 for location). Thin arrows indicate eroded edge of dune field; thick arrows show wind direction. Image resolution, 35 m per pixel; solar illumination angle, 26.4°.

personal communication, 1982). Slight differences in calculated surface slope and elevation measurements obtained from Goldstone and Arecibo elevation profiles may result from differing cell sizes because the observations represent an average for the entire cell.

The large collapse area at the shield summit that was first recognized from photogeologic analysis appears on radar profile c (Figure 13) to be about 400 m deep. The floor of this depression lies at an elevation close to that of the old cratered plateau west of Syrtis Major. The slope on the west wall of the depression is about 0.3°, whereas on the flanks of caldera C_1, slopes are about 1.4°. Along profile c, the slope on the surface of the shield to the west is about 0.2°, measured from a point immediately west of caldera C_1 to longitude 297°; the surface elevation then levels off until the shield overlaps the cratered plateau surface at longitude 299° (Figure 13). East of the depressed summit area, the surface slope on the shield is nearly level to longitude 288°; from longitude 288° to 284° it slopes about 0.25° east (profile c, Figure 13). From longitude 284° to the floor of Isidis Planitia,

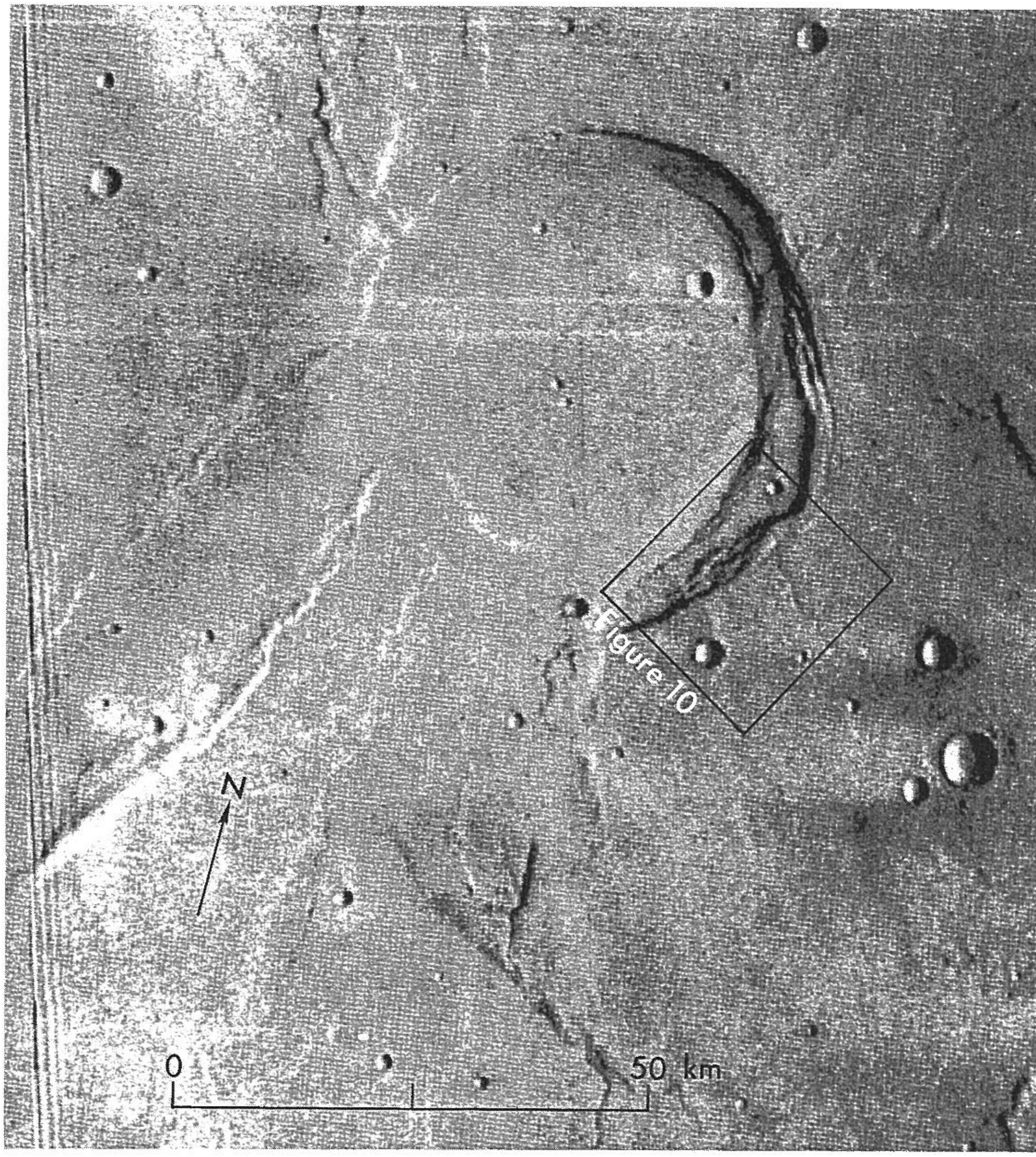

Fig. 7. Part of Viking orbiter image 375S32, enlarged to show summit caldera C_2. Footprint of Figure 10 indicated. Image resolution, 230 m per pixel; solar illumination angle, 21°.

the average slope increases significantly to 0.8°. Integration of the radar cell may cause the slopes of the radar profiles to be underestimated, especially at such localized surfaces like the flanks of caldera C_1, where local changes in elevation may be substantial.

DISCUSSION

The volcanic history of Syrtis Major began some time after the impact event that created the Isidis basin; it terminated at about the time that the earliest volcanic materials were deposited in Tharsis Montes, a period concurrent with the final stages of volcanism at Syria Planum, Lunae Planum, Alba Patera, and Hesperia Planum [*Scott and Carr,* 1978; *Scott and Tanaka,* 1981, *Scott,* this issue]. *Simpson et al.* [1982] suggested that volcanism at Syrtis Major may be associated with the ring of concentric fractures (e.g., Nili Fossae, Figure 13, profile g) that formed during the Isidis impact event; fracturing of this region by the Isidis impact event may have predisposed the surface to shallow partial melting and volcanism.

The absence of high-relief shields in Syrtis Major, Hesperia Planum, and the volcanic plains near Amphitrites Patera at latitude 59°S, longitude 299° [*Scott and Carr,* 1978] in the eastern hemisphere of Mars is in striking contrast to the giant shields of Tharsis Montes. The reasons for such different volcanic landforms may be related to changes in the composition (e.g., ultramafic to mafic; see *McGetchin and Smyth* [1978]), differentiation history, or eruptive styles of surface igneous rocks with time, thus, directly reflecting the thermal and chemical evolution of the interior. The absence of high-relief shields in the eastern hemisphere may also reflect differences in crustal thickness of that region since the height of a shield has implications regarding the depth of origin of the magma; *Eaton and Murata* [1960] have shown that the difference in density between the lava in its conduit and the surrounding rocks creates a hydrostatic head which

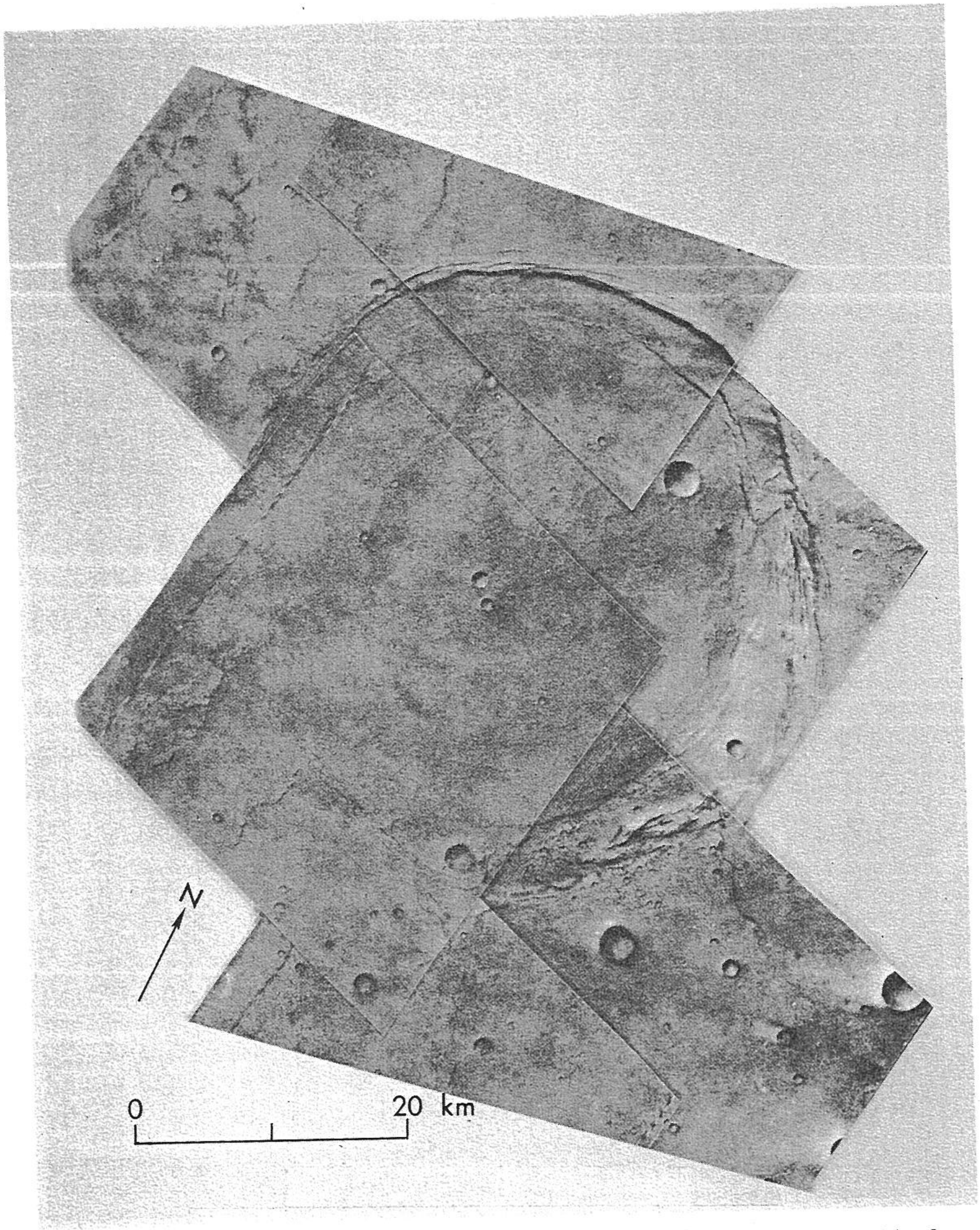

Fig. 8. Photomosaic of Viking orbiter images 716A18–716A23 showing summit caldera C_2 in Syrtis Major. Image resolution, about 34 m per pixel; solar illumination angle, about 24°.

limits shield height. No reliable values exist at present for actual crustal thicknesses on Mars, although extrapolations based on Mariner 9 gravity data and a single seismic event at Viking Lander 2 [*Eberhart,* 1977] indicates that the crust at Syrtis Major, Hesperia Planum, and Amphitrites Patera may be considerably thinner than it is beneath the crest of Tharsis Montes but not significantly different from the thickness under Olympus Mons (a high-relief shield) or Alba Patera (a low-relief shield). Differences between eruptive histories and style of volcanic landforms in Tharsis Montes and the older volcanic plains in the Martian eastern hemisphere are most likely the result of large-scale thermal perturbations of the mantle at Tharsis and local lithospheric weakening related to the creation of basins by impact in the eastern hemisphere.

The low average slopes (0.2°) on the flanks of the Syrtis Major shield are about 7 times shallower than the flattest shields on Earth, like Erta Ale and Mat'Ale in Ethiopia [*Pike and Clow,* 1981]. By comparison, the slopes on the flanks of Mauna Loa in Hawaii and Olympus Mons on Mars both average about 4°. *Wu et al.* [1982] have found, however, that

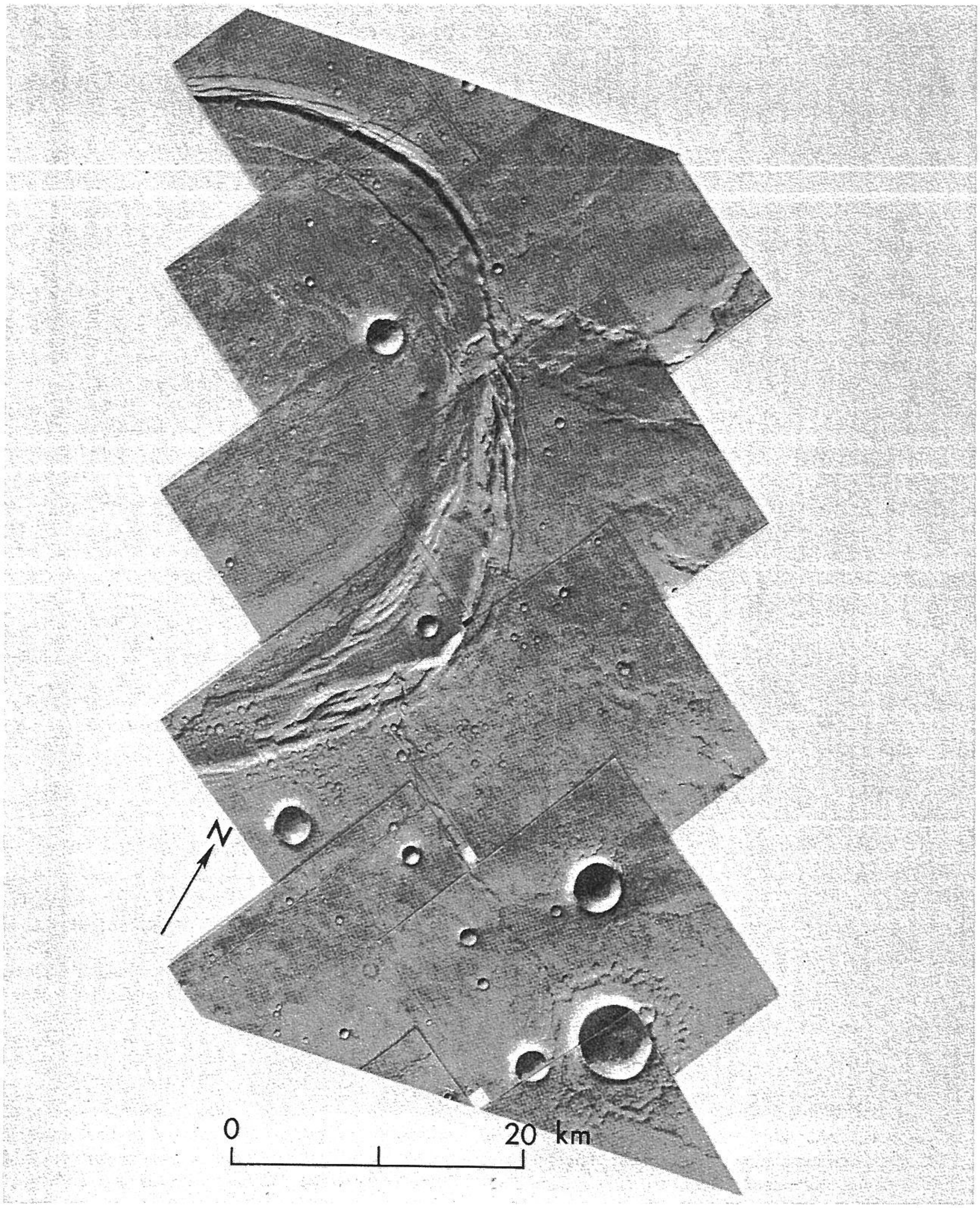

Fig. 9. Photomosaic of highest resolution Viking orbiter images of summit caldera C_2. Viking orbiter images include 716A46–716A57. Note intersection of caldera wall with 'wrinkle ridge' on east side and rough surface texture in center of caldera floor. Average image resolution, about 22 m per pixel; average solar illumination angles, about 24°.

are most
is of the
elated to
isphere.
ne Syrtis
e flattest
pia [*Pike*
flanks of
ars both
ver, that

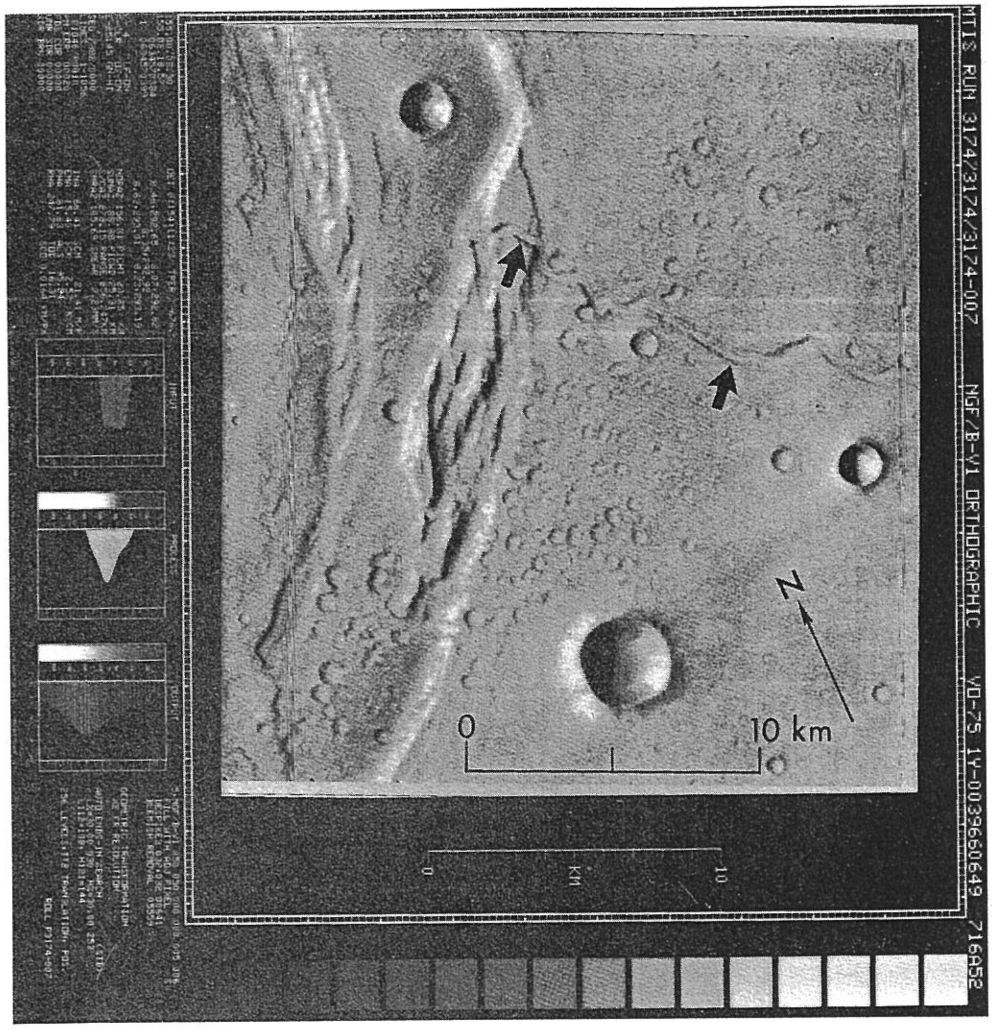

Fig. 10. Viking orbiter image 716A52 showing details of a lava channel (arrow) that extends radially from southeast rim of caldera C_2.

Olympus Mons does not have a simple shield profile: slopes range from 2° to 3° at elevations between 2 and 7 km above datum, from 8° to 24° at elevations of 7 to 16 km, and from 2.5° to 6.5° at elevations above 13 km.

The volume of the entire Syrtis Major shield is estimated in this study to be 0.2×10^6 km^3 on the basis of the radar elevation profiles and assuming that the edifice was constructed on the cratered plateau surface that is exposed immediately to the west (Figure 13). By comparison, the total volume (above 5-km elevation) of Olympus Mons has been estimated to be 2.59×10^6 km^3 [*Wu et al.*, 1982]. The Syrtis Major shield, which is approximately 1100 km in diameter, has an estimated maximum height of only 0.5 km. Olympus Mons, by comparison, has a maximum basal diameter of 580 km and a height of 24.6 km [*Wu et al.*, 1982]. *Pike and Clow* [1981] have recently determined the average volumes for several classes of Martian volcanoes, including montes (5.0×10^5 km^3), tholi (16×10^3 km^3), and paterae (10×10^3 km^3). The volume of an individual edifice within a given class can, however, overlap that of an edifice in a different class. The average volumes of large lava shields on Earth were calculated by *Pike and Clow* [1981] according to six classes of structures; estimated volumes for these large terrestrial shields range from 12×10^3 km^3 for oceanic (Hawaiian) shields that have small summit calderas and are predominantly tholeiitic in composition to 10 km^3 for submarine (seamount) shields with a large summit caldera and a dominantly tholeiitic composition with some alkalic basalt and alkalic differentiates.

At Syrtis Major there is little doubt that tectonic uplift played little or no role in shaping the present topography; the shield is totally constructional. It is not known why volcanism shut down at Syrtis Major; cessation was most likely related to a change in conditions within the mantle that were associated with the onset of thermal perturbations beneath the Tharsis region. Whatever the cause(s), subsequent volcanic activity on Mars (e.g., at Elysium and Tharsis) was characterized by an entirely new eruptive style—one in which stable sources of magma and continuing major crustal stresses allowed volcanism to persist for several eons.

It is now certain, from its physiographic setting and from radar-derived elevation data, that Syrtis Major is a 'planum' (plateau) and not a 'planitia' (low plain), contrary to its portrayal on the published maps of Mars [*Scott and Carr,*

Fig. 11. Enlarged section of Viking orbiter image 375A12 showing details of lava flow fronts (arrows) northwest of caldera C_1 (see Figure 2 for location). Image resolution, 220 m per pixel; solar illumination angle, 27°.

large
:eanic
ıd are
ıbma-
and a
basalt

uplift
y; the
volca-
likely
were
neath
t vol-
) was
ne in
rustal
.
from
ınum'
to its
Carr,

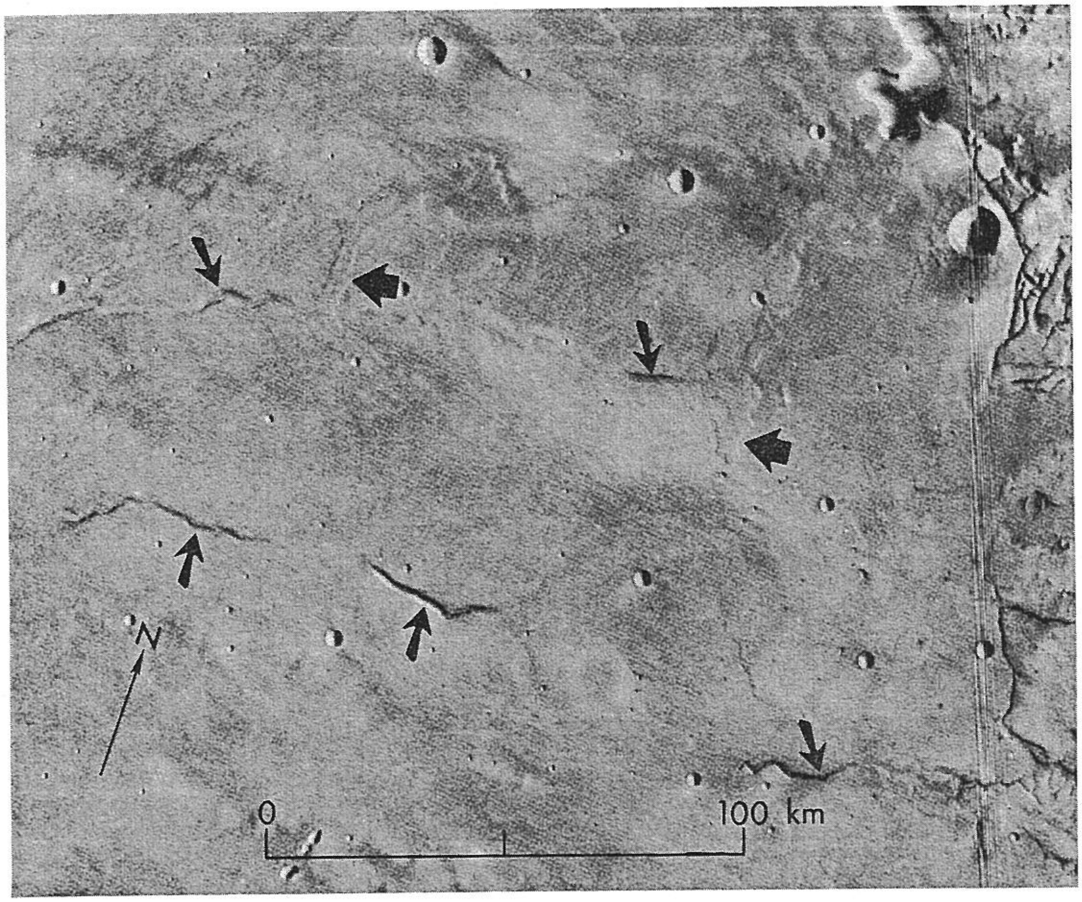

Fig. 12. Enlarged section of Viking orbiter image 377S53 showing a lava channel or collapsed lava tube (upper thin arrows) and a fissue vent (lower thin arrows) that are the sources of lava flows (wide arrows) located 650 km northeast of summit caldera C_1 (see Figure 2 for location). Surface slope in this area is 0.7° to east, toward Isidis Planitia.

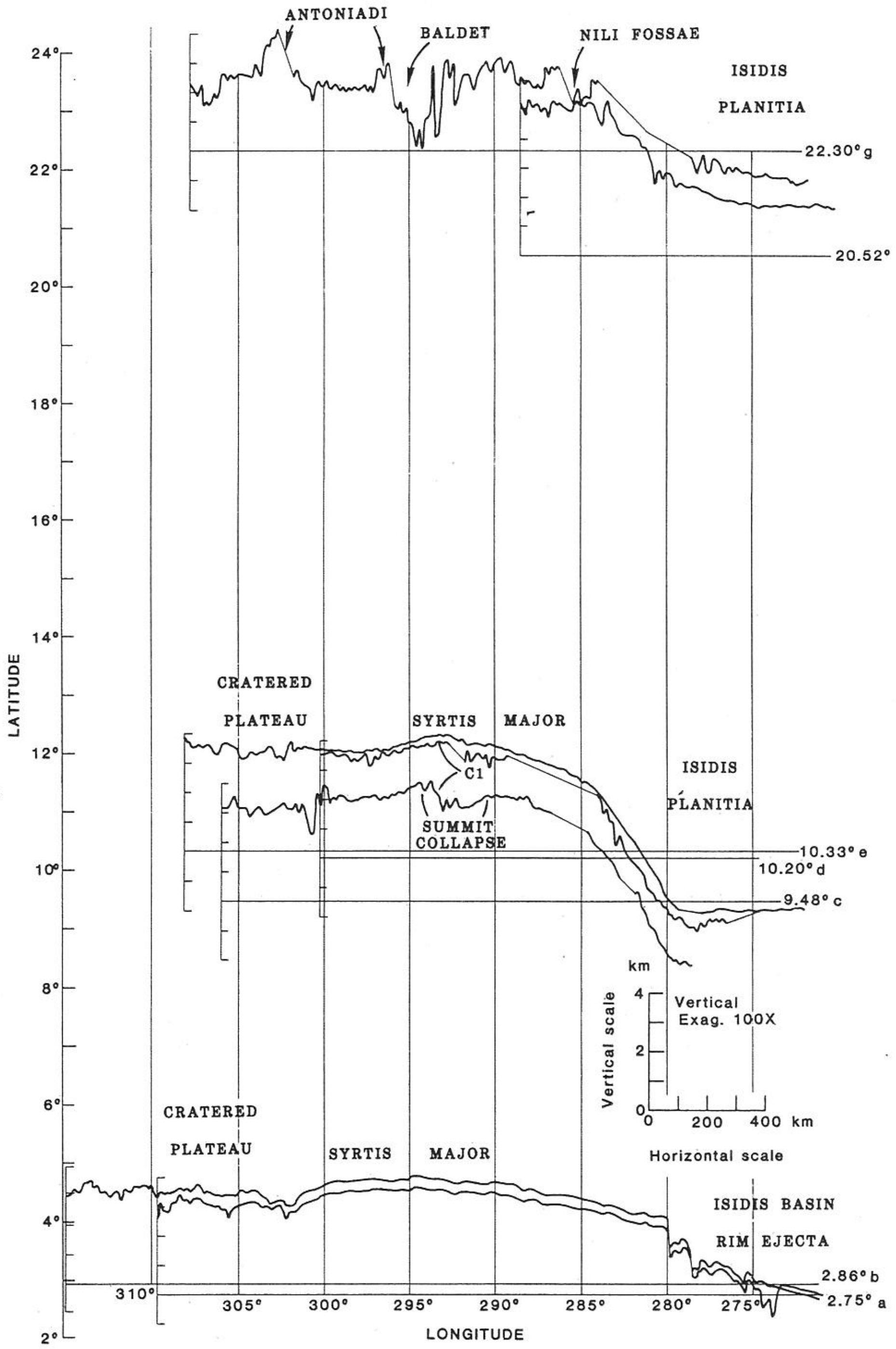

Fig. 13. Earth-based radar elevation profiles across Syrtis Major. Profiles e and f were obtained at Arecibo National Ionospheric Observatory in 1978 and 1980, respectively. (Data courtesy of J. Harmon, Arecibo, Puerto Rico). Profiles a and b were obtained at the Goldstone Tracking Facility in 1975, and profiles c, d, and g in 1978. (Data courtesy of G. Downs, Jet Propulsion Laboratory, Pasadena, California) Vertical resolution, about 150 m; horizontal resolution for both data sources is determined by size of radar cell on the surface (at subradar point), discussed in text. Vertical exaggeration, 100×. Thin straight-line segments on profiles indicates areas of missing information. Baselines of each profile are at zero elevation (6.1 mbar pressure).

1978; *U.S. Geological Survey,* 1976]. The 3- to 4-km elevation at Syrtis Major, the virtual absence of any recognizable rim of mountainous ejecta [*Meyer and Grolier,* 1977; *Schaber,* 1977] similar to features associated with other impact basins, and the absence of a gravity anomaly over this region [*Sjogren,* 1979] like the anomaly associated with Isidis Planitia strongly suggest that no impact basin existed at this site before the onset of volcanism [*Schaber et al.,* 1981].

Acknowledgments. I am indebted to K. L. Tanaka for his help in determining surface crater count statistics. This research was supported by National Aeronautics and Space Administration contract W13,709.

REFERENCES

Antoniadi, E. M., *La Planete Mars,* Hermann, Paris, 1930.

Belton, M. J. S., and D. M. Hunten, Spectrographic detection of topographic features on Mars, *Science, 166,* 225–227, 1969.

Belton, M. J. S., and D. M. Hunten, The distribution of CO_2 on Mars: A spectroscopic determination of surface topography, *Icarus, 15,* 204–232, 1971.

Breed, C. S., M. J. Grolier, and J. F. McCauley, Morphology and distribution of common 'sand' dunes on Mars: Comparison with the earth, *J. Geophys. Res., 84,* 8183–8203, 1979.

Capen, C. F., Jr., Martian albedo feature variations with season: Data of 1971 and 1973, *Icarus, 28,* 213–230, 1976.

De Vaucouleurs, G., *Physics of the Planet Mars,* Farber and Farber, London, 1954.

Downs, G. S., R. R. Green, and P. E. Reichley, Radar studies of the Martian surface at centimeter wavelengths: The 1975 opposition, *Icarus, 33,* 441–453, 1978.

Eaton, J. P., and K. J. Murata, How volcanoes grow, *Science, 132,* 925–938, 1960.

Eberhart, J., The skin of Mars, *Sci. News, 112,* 140–141, 1977.

Frey, H., Surface features on Mars: Ground-based albedo and radar compared with Mariner 9 topography, *J. Geophys. Res., 79,* 3907–3916, 1974.

Goldstein, R. M., W. G. Melbourne, G. A. Morris, G. S. Downs, and D. A. O'Handley, Preliminary radar results of Mars, *Radio Sci., 2,* 475–478, 1970.

Greeley, R., and P. D. Spudis, Volcanism on Mars, *Rev. Geophys. Space Phys., 19,* 13–42, 1981.

Hord, C. W., K. E. Simmons, and L. K. McLaughlin, Mariner 9 ultraviolet spectrometer experiment: Pressure-altitude measurements on Mars, *Icarus, 21,* 292–302, 1974.

McGetchin, T. R., and J. R. Smyth, The mantle of Mars: Some possible geological implications of its high density, *Icarus, 34,* 512–536, 1978.

Meyer, J. D., and M. J. Grolier, Geologic map of the Syrtis Major quadrangle of Mars, *U.S. Geol. Surv. Misc. Invest. Ser., Map I-995,* scale 1:5,000,000, 1977.

Pike, R. J., and G. D. Clow, Revised classification of terrestrial volcanoes and catalog of topographic dimensions with new results on edifice volume, *U.S. Geol. Surv. Open File Rep., 81-103,* 840 pp., 1981.

Pollack, J. B., and C. Sagan, Secular changes and dark-area regeneration on Mars, *Icarus, 6,* 434–439, 1967.

Pollack, J. B., and C. Sagan, Studies of the surface of Mars (very early in the era of spacecraft reconnaissance), *Radio Sci., 5,* 443–464, 1970.

Rogers, A. E. E., M. E. Ash, C. C. Councelman, I. I. Shapiro, and G. H. Pettengill, Radar measurement of the surface topography and roughness of Mars, *Radio Sci., 5,* 465–473, 1970.

Sagan, C., and J. B. Pollack, Elevation differences on Mars, *J. Geophys. Res., 73,* 1373, 1968.

Sagan, C., J. Veverka, and P. Gierasch, Observational consequences of martian wind regimes, *Icarus, 15,* 253–278, 1971.

Schaber, G. G., Geologic map of the Iapygia quadrangle on Mars, *U.S. Geol. Surv. Misc. Invest. Ser., Map I-1020,* scale 1:5,000,000, 1977.

Schaber, G. G., K. C. Horstman, and A. L. Dial, Jr., Lava flow materials in the Tharsis region of Mars, *Proc. Lunar Planet. Sci. Conf., 9th,* 3433–3458, 1978.

Schaber, G. G., K. L. Tanaka, and J. K. Harmon, Syrtis Major revisited: A highland volcanic planum, not a planitia, in *Papers Presented to the Third International Colloquium on Mars,* pp. 223–225, Lunar and Planetary Institute, Houston, Tex., 1981.

Schultz, P. H., and H. Glicken, Impact crater and basin control of igneous processes on Mars, *J. Geophys. Res., 84,* 8033–8047, 1979.

Scott, D. H., Volcanoes and volcanic provinces: Martian western hemisphere, *J. Geophys. Res.,* this issue.

Scott, D. H., and M. H. Carr, Geologic map of Mars, *U.S. Geol. Surv. Misc. Invest. Ser., Map I-1083,* scale 1:25,000,000, 1978.

Scott, D. H., and K. L. Tanaka, Mars: Paleostratigraphic restoration of buried surfaces in Tharsis, *Icarus, 45,* 304–319, 1981.

Simpson, R. A., G. L. Tyler, J. K. Harmon, and A. R. Peterfreund, Radar measurement of small-scale surface texture, *Icarus, 49,* 258–283, 1982.

Sjogren, W. L., Mars gravity: High-resolution results from Viking orbiter 2, *Science, 203,* 1006–1009, 1979.

Slipher, E. C., *A Photographic History of Mars, 1905–1961,* Lowell Observatory, Northland Press, Flagstaff, Ariz., 1962.

U.S. Geological Survey, Topographic map of Mars, U.S. Geol. Surv. in *Atlas of Mars, Topographic Ser. I-961,* Reston, Va., 1976.

Wells, R. A., Martian topography: Large scale variations, *Science, 166,* 862–866, 1969.

Wu, S. S. C., P. A. Garcia, R. Jordan, and F. J. Schafer, Quantitative analysis of Olympus Mons (abstract), Report of Planetary Geology Program, 1981, *NASA Tech. Memo, TM-84211,* 141–143, 1982.

(Received November 25, 1981;
revised March 29, 1982;
accepted May 14, 1982.)